THE JOURNAL OF NAVIGATION (2018), **71**, 1431–1440.
doi:10.1017/S037346331800036X

A TOA/AOA Underwater Acoustic Positioning System Based on the Equivalent Sound Speed

Mingzhen Xin[1,2], Fanlin Yang[1,2,3], Faxing Wang[1], Bo Shi[1,2,3], Kai Zhang[1,2,3] and Hui Liu[1]

[1](*College of Geomatics, Shandong University of Science and Technology, Qingdao 266590, China*)
[2](*Key Laboratory of Surveying and Mapping Technology on Island and Reef, National Administration of Surveying, Mapping and Geoinformation, Qingdao 266590, China*)
[3](*Key Laboratory of Marine Surveying and Charting in Universities of Shandong, Qingdao 266590, China*)
(E-mail: yang723@163.com)

High-precision underwater positioning must eliminate the influence of refraction artefacts. Since a Time Of Arrival - Global Navigation Satellite System Intelligent Buoys (TOA-GIB) system does not measure incident beam angles, common refraction correction methods cannot be directly used for refraction artefacts. An Equivalent Sound Speed (ESS) iteration method is proposed and is based on the transformation relations between depth, the ESS gradient and the incident beam angle. On this basis, a TOA/AOA-GIB system without a real-time Sound Speed Profile (SSP) is proposed to estimate the target position and the ESS gradient as unknown parameters. The results from a simulation experiment show that the positioning accuracy of a TOA/AOA-GIB system is better than 0·07% of water depth when the accuracy of the incident beam angle is 0·1°.

KEYWORDS

1. Underwater Acoustic Positioning. 2. Equivalent Sound Speed. 3. ESS Iteration Method. 4. TOA/AOA-GIB System. 5. Refraction Correction.

Submitted: 15 November 2017. Accepted: 2 May 2018. First published online: 5 June 2018.

1. INTRODUCTION. Underwater positioning is the basis of many marine development activities (Ballu et al., 2009; Ikuta et al., 2008; Niess, 2005). Acoustic positioning systems, such as Ultra Short Baseline (USBL), Short Baseline (SBL), Long Baseline (LBL) and Global Navigation Satellite System Intelligent Buoys (GIB) systems (Vickery, 1998; Thomas, 1998; Chen, 2013) are widely used, due to the good acoustic propagation characteristics of seawater. USBL uses Time Of Arrival (TOA) and Angle Of Arrival (AOA)

to position a target, which is operationally simple but has low accuracy. SBL, LBL and GIB systems all use TOA for distance intersection positioning, and the difference between them lies in the layout of the acoustic array. The acoustic array of a GIB system consists of a series of surface buoys whose exact location can be provided by a Global Navigation Satellite System (GNSS), which makes the GIB system advantageous in both operation and accuracy (Alcocer et al., 2006; Desset et al., 2003).

With the increasing maturity of underwater acoustic technology, measurement errors caused by system hardware have been effectively controlled and eliminated. At present, the main factor that restricts the accuracy of underwater acoustic positioning is refraction artefacts caused by the vertical changes of sound speed (Xu et al., 2005). When Sound Speed Profile (SSP) and incident beam angles have been measured, the refraction correction method is the direct way to remove refraction artefacts (Kammerer, 2000). However, those TOA positioning systems do not measure incident beam angles in real time, making it difficult to directly use the existing refraction correction method.

In addition, refraction artefacts can be eliminated by optimised localisation algorithms. For example, Xu et al. (2005) developed new data processing strategies for quantifying crustal deformation at the ocean floor: single- and double-difference methods. Yang et al. (2011) presented a new method of positioning underwater static objects, in which the ranging errors follow a quadratic relationship with the travel time of acoustic signals. However, these methods are difficult to apply to underwater dynamic positioning because of the lack of redundant observations.

This paper focuses on the problem of refraction correction in dynamic underwater positioning. An Equivalent Sound Speed (ESS) iteration method is proposed to eliminate the positioning error caused by refraction artefacts when SSP has been collected in a TOA-GIB system. Then, a TOA/AOA-GIB system without real-time SSP is proposed to estimate target position and ESS gradient as unknown parameters. Finally, the ESS iteration method and the TOA/AOA-GIB system are verified by simulation experiments.

2. ESS ITERATION METHOD OF TOA-GIB SYSTEM.

As shown in Figure 1(a), a TOA-GIB system consists of a set of surface buoys (reference points) with GNSS receivers, submerged hydrophones, and radio modems. The hydrophones receive the acoustic impulses emitted periodically by a synchronised pinger installed on the underwater target and the TOA is recorded and sent in real time through the radio link to a control unit. Because position estimates are only available at the control unit, this system is naturally suited for tracking applications.

The coordinates of reference points (x_i, y_i, z_i) $(i = 1, 2, \ldots n)$ can be provided by GNSS, where i stands for the reference point number. The system measures the travel time of acoustic signals t_i from the reference points to the target. Suppose sound speed c is constant, the distances between the reference points and the target are $\rho_i = ct_i$. Let the target coordinates be (x_t, y_t, z_t), then the observation equation is given as

$$\rho_i = \sqrt{(x_1 - x_i)^2 + (y_i - y_i)^2 + (z_i - z_i)^2} \tag{1}$$

The target coordinates (x_t, y_t, z_t) can be obtained by least square solution of Equation (1). However, refraction artefacts caused by the variation of sound speed c in a vertical direction will lead to a large positioning deviation.

https://doi.org/10.1017/S037346331800036X Published online by Cambridge University Press

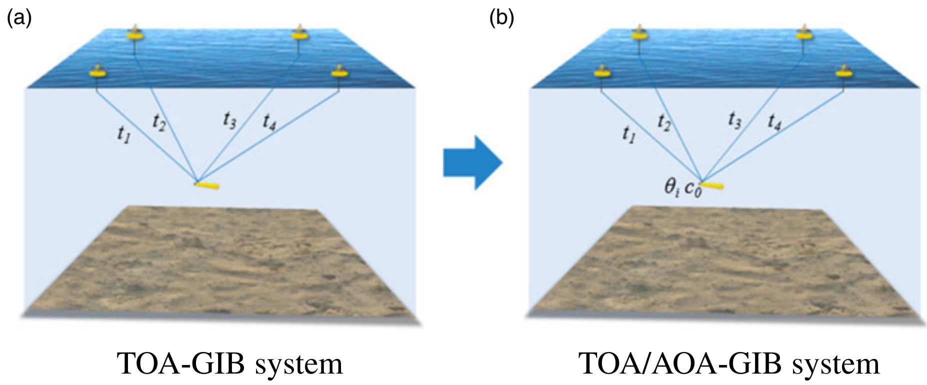

Figure 1. TOA-GIB system.

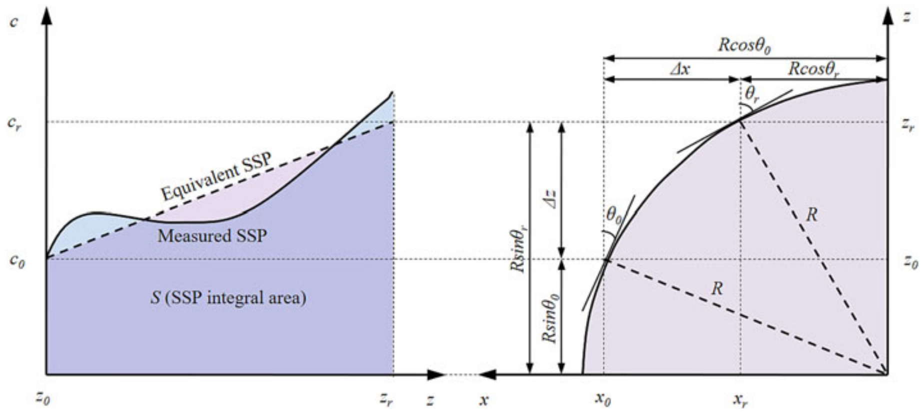

Figure 2. Equivalent sound speed method.

2.1. *Refraction correction.* As shown in Figure 2, according to the ESS method (Geng and Zielinski, 1999), let the SSP integral area between water depth z_0 and z_r be S and c_0, c_r are the sound speeds at depths of z_0, z_r. The ESS gradient g is given as

$$\begin{aligned} g &= (c_r - c_0)/(z_r - z_0) \\ &= 2S/(z_r - z_0)^2 - 2c_0/(z_r - z_0) \end{aligned} \tag{2}$$

The acoustic path in the constant gradient sound speed layer is a circular arc with radius $R = 1/pg$, the Snell constant p is given as (Kammerer, 2000)

$$p = \sin\theta_0/c_0 = \sin\theta_r/c_r \tag{3}$$

where θ_0 is the incident beam angle, and the emergent beam angle θ_r is (Lu et al., 2012)

$$\theta_r = 2\arctan[e^{tg}\tan(\theta_0/2)] \tag{4}$$

The vertical distance Δz and the plane distance Δx are given as follows

$$\Delta x = R(\cos\theta_0 - \cos\theta_r) \tag{5}$$

$$\Delta z = R(\sin\theta_r - \sin\theta_0) \tag{6}$$

https://doi.org/10.1017/S037346331800036X Published online by Cambridge University Press

The distance after refraction correction can be given by $\rho^2 = \Delta z^2 + \Delta x^2$. Obviously, the premise of the ESS method is that the incident beam angle θ_0 is known. However, the scalar hydrophone of a TOA-GIB system can only measure travel time of acoustic signals, so this refraction correction method cannot be directly applied to a TOA-GIB system.

2.2. *ESS iteration method.* Although a TOA-GIB system does not measure the incident beam angle θ_0, when the ESS gradient g, the travel time t and the target depth z_0 are known, a new equation can be obtained by substituting Equation (3) into Equation (4):

$$\tan[\arcsin(c_r \sin\theta_0/c_0)/2] = e^{tg}\tan(\theta_0/2) \tag{7}$$

In Equation (7), the incident beam angle θ_0 is an unknown parameter and can be solved by the Newton iteration method.

The positioning calculation procedure of the ESS iteration method is as follows:

(1) Calculate the initial distance $\rho_i^0 = c' t_i$, where c' is the approximation of sound speed which can be obtained from the measured SSP;
(2) Substitute the distance ρ_i^0 and the reference point coordinates (x_i, y_i, z_i) into Equation (1) to calculate the target approximate coordinates (x_t, y_t, z_t);
(3) Calculate the ESS gradient g_i with Equation (2);
(4) Substitute the ESS gradient g_i, the travel time t_i into Equation (7), to calculate the incident beam angle θ_{0i};
(5) Substitute the incident beam angle θ_{0i}, the ESS gradient g_i and the travel time t_i into Equations (3)∼(6), to calculate the corrected distance ρ_i;
(6) Repeat steps (2)–(5) until the change of target coordinates is less than the threshold ε_p.

3. TOA/AOA-GIB SYSTEM.

An ESS iteration method for a TOA-GIB system when the SSP is real-time and accurate is presented in Section 2. However, to derive real-time SSP information, an underway-profiling instrument is needed (Clarke et al., 2000). In most cases, it is of considerable inconvenience and high cost for an Autonomous Underwater Vehicle (AUV) to operate in underwater environments equipped with such an underway-profiling instrument (Zhang et al., 2016). To achieve high precision underwater dynamic positioning without a real-time SSP, an assumption is proposed: If the incident beam angles θ_{0i} and the real-time sound speed c_0 are measured, can the accurate estimation of the target position and the ESS gradient be achieved by iteration computation?

As shown in Figure 1(b), a TOA/AOA-GIB system is designed based on this assumption. The surface-buoys (reference points) are equipped with GNSS receivers and submerged transponders. A transceiver installed on the underwater target sends out the interrogation and receives the reply from the transponders. The vector hydrophone (Nehorai and Paldi, 1994; Tichavsky et al., 2001) of the transceiver records the incident beam angles θ_{0i} and the time of arrival t_i. The positions of the buoys are also available by coding within the acoustic emission pattern. A micro sound speed meter mounted on the transceiver is used to measure the real-time sound speed c_0. Unlike in a TOA-GIB system, the data position information is available at the control unit of the underwater platform, and therefore, the system can be directly used for navigation.

Since the heave of surface buoys caused by waves is usually very small compared to the target depth, it can be considered that the ESS gradients g_i between different reference

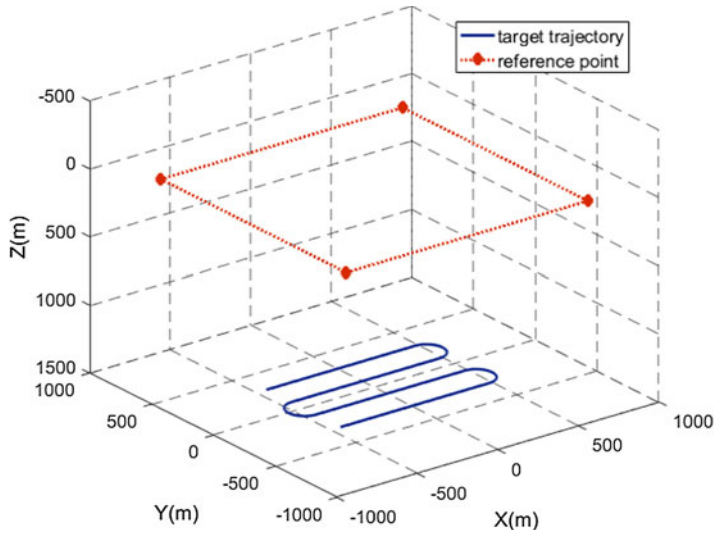

Figure 3. Reference points and target trajectory.

points and the target are approximately the same, that is, $g_i = g$. Therefore, the target position (x_t, y_t, z_t) and the ESS gradient g can be estimated as unknown parameters. To calculate g, a new equation can be obtained by substituting Equation (4) into Equation (5):

$$p\Delta xg + \cos\left[2\arctan(e^{tg}\tan(\theta_0/2))\right] - \cos\theta_0 = 0 \tag{8}$$

If we linearize Equation (8), and the error equation is given as follows

$$V = AX - L \tag{9}$$

where $A = [a_1\ a_2\ \cdots a_n]^T$, $L = [l_1\ l_2\ \cdots\ l_n]^{\mathrm{T}}$, and a_i, l_i are given as follows

$$a_i = p_i\Delta x_i - \frac{2t_i e^{t_i g}\tan(\theta_{0i}/2)}{1 + (e^{t_i g}\tan(\theta_{0i}/2))^2}\sin\left[2\arctan\left(e^{t_i g}\tan(\theta_{0i}/2)\right)\right] \tag{10}$$

$$l_i = \cos\theta_{0i} - p_i\Delta x_i g - \cos\left[2\arctan\left(e^{t_i g}\tan(\theta_{0i}/2)\right)\right] \tag{11}$$

The least square solution of Equation (8) is:

$$X = \left(A^T A\right)^{-1} A^T L \tag{12}$$

The positioning calculation procedure of the TOA/AOA-GIB system is:

(1) Calculate the initial distance $\rho_i^0 = c' t_i$, where t_i is measured by the vector hydrophone, and c_0 is measured by the micro sound speed meter;
(2) Substitute the distance ρ_i^0 and the reference point coordinates (x_i, y_i, z_i) into Equation (1) to calculate the approximate target coordinates (x_t, y_t, z_t);
(3) Substitute the incident beam angle θ_{0i}, the travel time t_i and the sound speed c_0 into Equations (8)~(12), to calculate the approximate ESS gradient g;

https://doi.org/10.1017/S037346331800036X Published online by Cambridge University Press

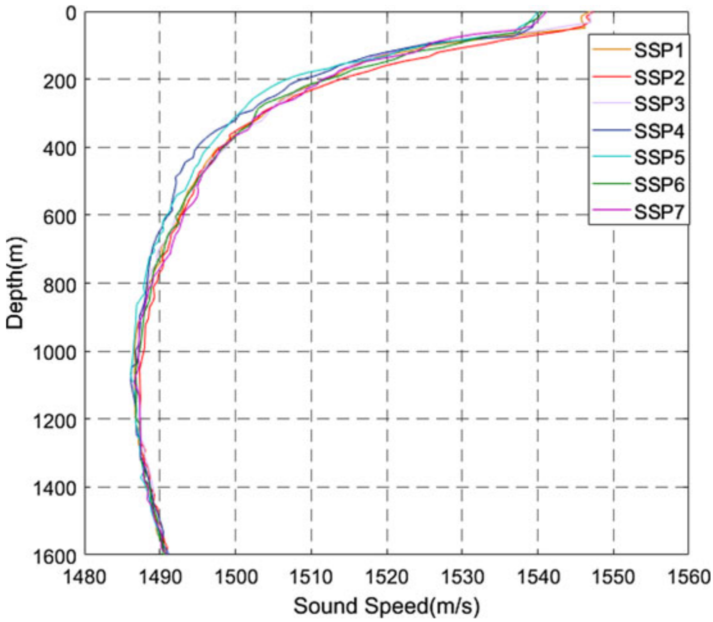

Figure 4. Sound speed profile.

(4) Substitute the incident beam angle θ_{0i}, the ESS gradient g and the travel time t_i into Equations (3)∼(6), to calculate the corrected distance ρ_i;
(5) Repeat steps (2)–(4) until the change of target coordinate is less than the threshold ε_p.

4. EXPERIMENT AND ANALYSIS. An experiment was designed to verify the ESS iteration method and the TOA/AOA-GIB system. The major purpose of this experiment was twofold: (1) The SSPs collected in the South China Sea are used for a positioning simulation. It is assumed that one of the SSPs is the real-time SSP, and the other SSPs are non-real-time SSPs. The ESS iteration method is used to eliminate the influence of refraction artefacts, to verify the calculation accuracy of the ESS iteration method, and to test the effect of the temporal and spatial variation of the SSP on the positioning accuracy. (2) The TOA/AOA-GIB system is used for the positioning simulation to verify whether the novel system can eliminate the systematic error due to the non-real-time SSP, and the influence of the incident beam angle error on the positioning accuracy is tested.

As shown in Figure 3, the reference points are laid in a square with sides of length 1,500 m. The underwater target moves along the S-shaped route at a depth of $z = 1,500$ m. As shown in Figures 4 and 5, a set of SSPs are collected in the South China Sea. SSP2 is assumed to be an accurate real-time speed profile. Suppose the random heaves of reference points are less than 5 m. The random error of the travel time is assumed to be $\Delta t = 10\,\mu$s, and the random error of reference point coordinates are assumed to be $\Delta P_x = 0{\cdot}1$ m, $\Delta P_y = 0{\cdot}1$ m, $\Delta P_z = 0{\cdot}1$ m. In addition, the random error of sound speed is $\Delta c_0 = 0{\cdot}02$ m/s, and the random error of incident beam angle is $\Delta\theta_0$. Standard deviation is used as an indicator

https://doi.org/10.1017/S037346331800036X Published online by Cambridge University Press

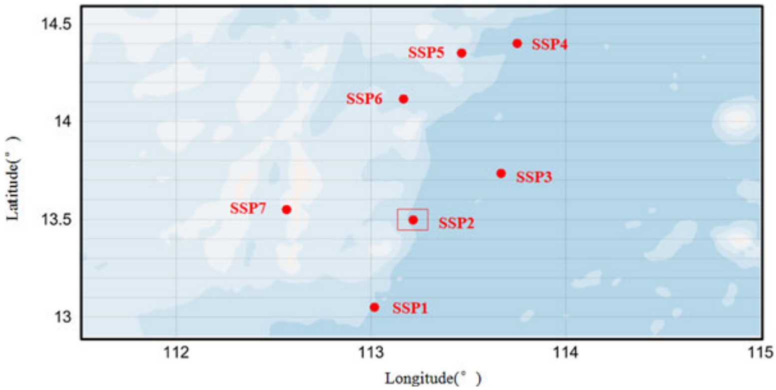

Figure 5. Distribution of sound speed profile.

Table 1. Standard deviation of target coordinate (the ESS iteration method).

	SSP1	SSP2	SSP3	SSP4	SSP5	SSP6	SSP7
σ_{Ph}^{e} (m)	0·50	0·10	0·46	1·11	1·18	0·50	0·47
σ_{Pv}^{e} (m)	1·14	0·14	1·03	2·80	2·98	1·15	1·06
σ_{g}^{e} (s^{-1})	0·00034	0·00001	0·00163	0·00567	0·00635	0·00726	0·00676
$\sigma_{\theta 0}^{e}$ (°)	0·03900	0·00368	0·04367	0·11108	0·09869	0·04198	0·03157

Table 2. Standard deviation of target coordinate (the TOA/AOA-GIB system).

	$\Delta\theta_0 = 0{\cdot}01°$	$\Delta\theta_0 = 0{\cdot}025°$	$\Delta\theta_0 = 0{\cdot}04°$	$\Delta\theta_0 = 0{\cdot}055°$	$\Delta\theta_0 = 0{\cdot}07°$	$\Delta\theta_0 = 0{\cdot}085°$	$\Delta\theta_0 = 0{\cdot}1°$
σ_{Ph}^{s} (m)	0·20	0·22	0·25	0·28	0·32	0·36	0·41
σ_{Pv}^{s} (m)	0·23	0·30	0·39	0·49	0·59	0·70	0·82
σ_{g}^{s} (s^{-1})	0·00019	0·00026	0·00035	0·00045	0·00056	0·00067	0·00078

of calculated results:

$$\sigma = \sqrt{\sum_{i=1}^{n} (\beta_e - \beta)^2 / n} \tag{13}$$

where β_e is the estimation of the parameter, and β is the true value of the parameter.

4.1. *Experiment results.* The experiment was divided into two steps. First, using the ESS iteration correction method, the target coordinates are calculated. σ_{Ph}^{e} and σ_{Pv}^{e} represent the standard deviations of the target plane coordinates and the vertical coordinate, respectively. $\sigma_{\theta 0}^{e}$ and σ_{g}^{e} are the standard deviations of the incident beam angle and the ESS gradient, respectively. Then, the TOA/AOA-GIB system is used to discover the target location. σ_{Ph}^{s}, σ_{Pv}^{s}, σ_{g}^{s} represent the standard deviations of the target plane coordinate, the vertical coordinate, and the ESS gradient. Statistical results of standard deviations are shown in Tables 1 and 2. Error curves of the incident beam angle, the target coordinates and the ESS gradient are shown in Figures 6, 7 and 8.

4.2. *Experiment analysis.* As shown in Table 1, when the ESS iteration method with SSP2 is used for the positioning calculation, σ_{Ph}^{e} and σ_{Pv}^{e} are all decimetre-scale, which indicates that the ESS iteration method can use a real-time and exact SSP to eliminate the

https://doi.org/10.1017/S037346331800036X Published online by Cambridge University Press

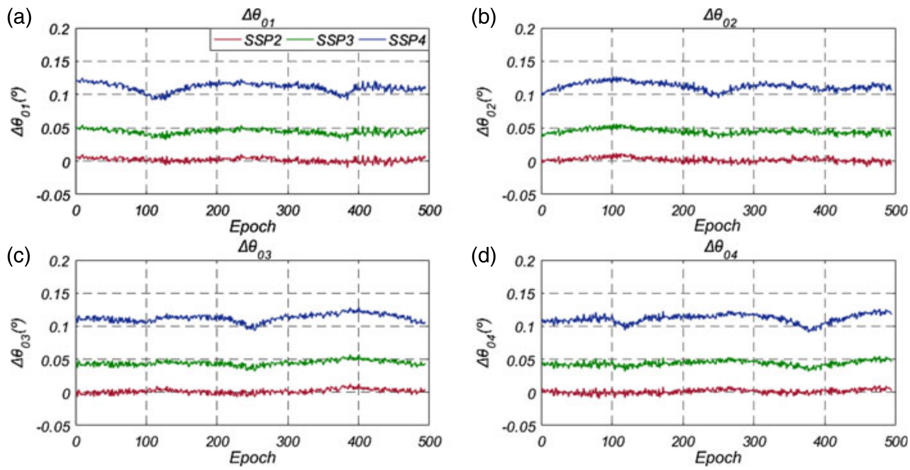

Figure 6. Beam incident angle error curves ((a) $\Delta\theta_{01}$; (b) $\Delta\theta_{02}$; (c) $\Delta\theta_{03}$; (d) $\Delta\theta_{04}$).

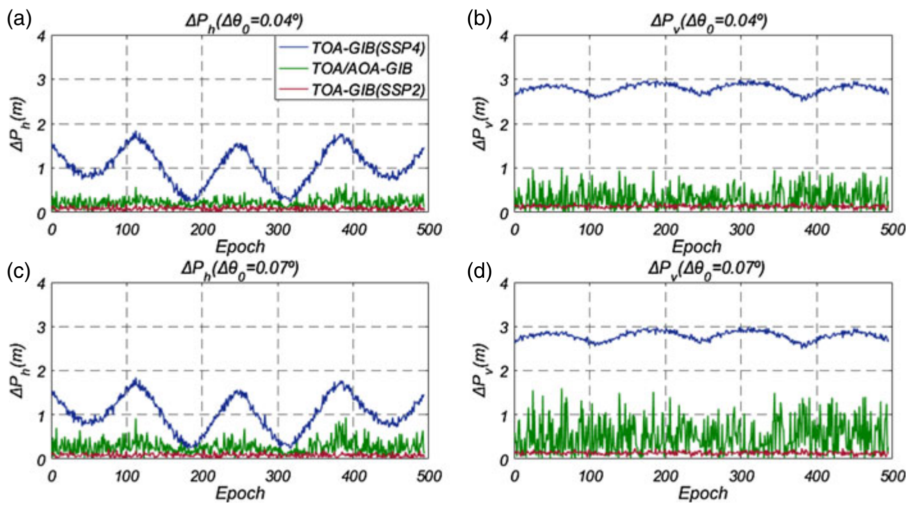

Figure 7. Target coordinate error curves ((a) $\Delta P_h(\Delta\theta_0 = 0{\cdot}04^\circ)$; (b) $\Delta P_v(\Delta\theta_0 = 0{\cdot}04^\circ)$; (c) $\Delta P_h(\Delta\theta_0 = 0{\cdot}07^\circ)$; (d) $\Delta P_v(\Delta\theta_0 = 0{\cdot}07^\circ)$).

influence of refraction artefacts. However, as shown in Figures 6 and 7, when the SSP is inaccurate, there are systematic errors in both the incident beam angle and the target coordinates. Therefore, the real-time SSP is very important for high precision underwater positioning and navigation.

As shown in Table 2 and Figures 7 and 8, systematic errors are effectively suppressed in the TOA/AOA-GIB system. Although the positioning accuracy becomes worse with the increase of $\Delta\theta_0$, when $\Delta\theta_0$ is $0{\cdot}1^\circ$, the standard deviation between the coordinates in the TOA/AOA-GIB system is at the decimetre level, which is better than 0·07% of water depth. Therefore, the TOA/AOA-GIB system can achieve high-precision dynamic positioning, with a sound speed sensor reading c_0, but without a real-time SSP.

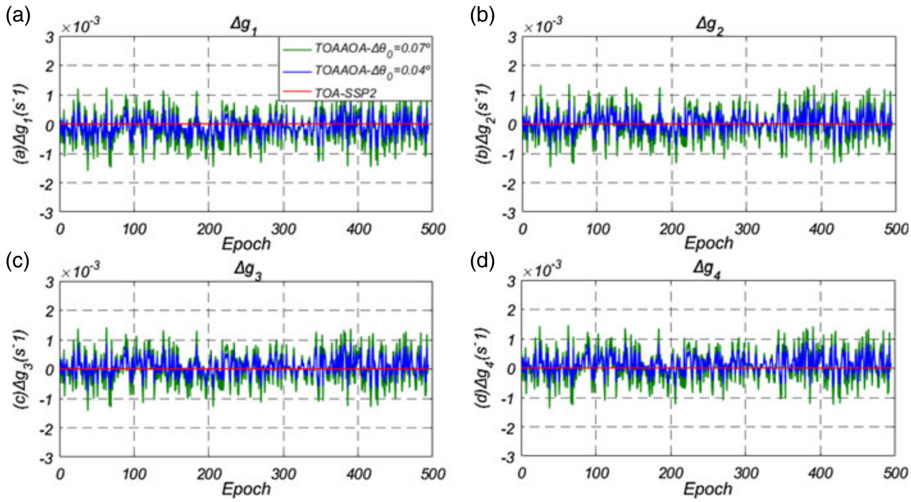

Figure 8. ESS gradient error curves ((a) Δg_1; (b) Δg_2; (c) Δg_3; (d) Δg_4).

5. CONCLUSION.

Since incident beam angles are not measured in the TOA-GIB system, commonly used refraction correction methods are no longer applicable; thus, an ESS iteration method is proposed to reduce the influence of refraction artefacts. On this basis, a TOA/AOA-GIB system for high precision dynamic positioning is proposed, in which incident beam angles are used as observations to calculate target coordinates and ESS gradient. Experimental results show that the positioning accuracy of the TOA/AOA-GIB system is better than 0·07% of water depth when the angle measurement accuracy is better than 0·1°. Since this is comparable with the angle measurement accuracy of USBL (0·1°), it is considered that the TOA/AOA-GIB system has certain research value and practical significance.

ACKNOWLEDGMENTS

This work is supported by National Key R&D Program of China (grant Nos. 2016YFB0501700, 2016YFB0501705) and Shandong Provincial Key R&D Program (grant No. 2018GHY115002).

REFERENCES

Alcocer, A., Oliveira, P. and Pascoal, A. (2006). Underwater acoustic positioning systems based onbuoys with GPS. *Proceedings of the Eighth European Conference on Underwater Acoustics, 8th ECUA, Carvoeiro, Portugal, June 12–15*.

Ballu, V., Ammann, J., Pot, O., Viron, O. D., Sasagawa, G. S. and Reverdin, G. (2009). A seafloor experiment to monitor vertical deformation at the Lucky Strike volcano, Mid-Atlantic Ridge. *Journal of Geodesy*, **83**, 147–159.

Desset, S., Damus, R., Morash, J. and Bechaz, C. (2003). Use of GIBs in AUVs for underwater archaeology. *Sea Technology*, **44**(12), 22.

Geng, X. and Zielinski, A. (1999). Precise multibeam acoustic bathymetry. *Marine Geodesy*, **22**, 157–167.

Clarke, E. H., Lamplugh, M. and Kammerer, E. (2000). Integration of near-continuous sound speed profile information. *Paper read at Canadian Hydrographic Conference, Proceedings CDROM, Victoria, Canada*.

Ikuta, R., Tadokoro, K., Ando, M., Okuda, T., Sugimoto, S. and Takatani, K. (2008). A new GPS-acoustic method for measuring ocean floor crustal deformation: Application to the Nankai trough. *Journal of Geophysical Research*, **113**(2), 229–234.

Kammerer, E. (2000). *New method for the removal of refraction artifacts in multibeam echosounder systems*. PhD Thesis. University of New Brunswick, Canada.

Lu, X., Bian, S., Huang, M. and Zhai, G. (2012). An improved method for calculating average sound speed in constant gradient sound ray tracing technology. *Geomatics & Information Science of Wuhan University*, **37**(5), 590–593.

Nehorai, A. and Paldi, E. (1994). Acoustic vector sensor array processing. *IEEE Transactions on Signal Processing*, **42**(9), 2481–2491.

Niess, V. (2005). Underwater acoustic positioning in ANTARES. *Proceedings of the 29th International Cosmic Ray Conference, Pune, India, August 3–10*.

Thomas, H. (1998). GIB buoys: an interface between space and depths of the oceans. *Proceedings of the Workshop on Autonomous Underwater Vehicles, Cambridge, Massachusetts, USA, August 20–21*. IEEE.

Tichavsky, P., Wong, K. T. and Zoltowski, M. D. (2001). Near-field/far-field azimuth and elevation angleestimation using a single vector hydrophone. *IEEE Transactions on Signal Processing*, **49**(2), 2498–2510.

Vickery, K. (1998). Acoustic positioning systems. New concepts-the future. *Workshop on Autonomous Underwater Vehicles, IEEE*, 103–110.

Xu, P., Ando, M. and Tadokoro, K. (2005). Precise, three-dimensional seafloor geodetic deformationmeasurements using difference techniques. *Earth Planets Space* **57**, 795–808.

Yang, F., Lu, X., Li, J., Han, L. and Zheng, Z. (2011). Precise positioning of underwater static objects without sound speed profile. *Marine Geodesy*, **34**(2), 138–151.

Chen, H. (2013). The estimation of angular misalignments for ultra-short baseline navigation systems. Part II: experimental results. *Journal of Navigation*, **66**(5), 773–787.

Zhang, K., Li, Y., Zhao, J. and Rizos, C. 2016. Underwater navigation based on real-time simultaneous sound speed profile correction. *Marine Geodesy*, **39**(1), 98–111.